SHIPPING TO AMERICA

XIWEN BAI
Tsinghua University

JESÚS FERNÁNDEZ-VILLAVERDE
University of Pennsylvania

YILIANG LI
University of International Business and Economics

RICARDO MARTO
Federal Reserve Bank of St. Louis

FRANCESCO ZANETTI
University of Oxford

October 2025

We study the evolution of containerized shipping to the United States and its implications for trade disruptions. Using high-frequency satellite data covering all U.S.-bound container vessels between 2017 and 2025, we document new facts on capacity allocation across the major routes and construct measures of disruptions from port congestion, canal bottlenecks, and rerouting associated with security threats. To interpret these patterns and quantify their implications, we develop a multi-route general equilibrium model in which shipping firms choose sailing speeds, load factors, and capacity allocations. Calibrated to micro data, the model replicates observed trends. The model is then used to quantify the macroeconomic impact of our underlying estimates of U.S.-bound shipping disruptions.

KEYWORDS: container ships, satellite data, shipping capacity, shipping disruptions, shipping routes, tariffs

JEL CLASSIFICATION: E23, L91, O18, O41, R40.

Xiwen Bai: xiwenbai@tsinghua.edu.cn
Jesús Fernández-Villaverde: jesusfv@sas.upenn.edu
Yiliang Li: yiliang_li@uibe.edu.cn
Ricardo Marto: ricardo.marto@stls.frb.org
Francesco Zanetti: francesco.zanetti@economics.ox.ac.uk

1. INTRODUCTION

Over the past few years, a sequence of high-profile disruptions has exposed critical vulnerabilities in the global shipping sector. The COVID-19 pandemic, the blockage of the Suez Canal in 2021, the Red Sea crisis in 2023 and 2024, and renewed tensions in the Strait of Hormuz in 2025 have triggered sharp delays, soaring costs, and ripple effects across global supply chains. Yet most economic models treat the shipping sector as a passive intermediary. This paper asks: How do strategic responses by shipping firms—through capacity reallocation and pricing—mediate the impact of global disruptions on U.S. imports?

We answer this question by combining new micro data with a general equilibrium model of shipping. We begin by assembling a new dataset that tracks the universe of container vessels arriving at U.S. ports between January 2017 and March 2025 (Section 2). We leverage real-time high-frequency satellite-based records from the Automatic Identification System (AIS) to measure potential shipping supply across U.S.-bound routes. Six major routes originating in Asia, Europe, the Middle East, and South America are considered. Our evidence shows that the post-2020 shipping boom was not a uniform expansion: capacity surged overall at the expense of other regions but was disproportionately reallocated to the Asia-West Coast route.

We then quantify disruptions stemming from port congestion, bottlenecks at the Panama Canal and Suez Canal, and rerouting associated with security threats and propose measures of effective shipping supply by major trade route (Section 3). Port congestion noticeably reduced shipping supply along the Asia to West Coast route in 2021, when container ships waited more than 60 hours offshore before being able to unload. Canal bottlenecks have been slowly rising over time in particular in the Panama Canal, where ships average a waiting time of 40 hours to cross the canal—almost double what it was in 2017 and 2019. The rerouting of vessels away from the Suez Canal to the Cape of Good Hope is visible starting in 2024, adding between 800 to 1,200 nautical miles to the average journey from Asia or the Middle East. These episodes reduced potential capacity by as much as 20 percentage points in 2021 along the Asia to West Coast route and by 40 percentage points in 2024 along the Asia to East Coast route via the Suez Canal.

To interpret these patterns and quantify their aggregate implications, we develop a multi-region, multi-route general equilibrium model in which shipping firms allocate capacity across routes, choose sailing speeds, loading factors, and set prices (Section 4). Retailers choose where to source imports based on route-level prices and idiosyncratic taste shocks, and consumers choose between domestic and imported varieties. The model nests key features of the shipping industry and is disciplined by observed AIS data on vessel flows, speed, and route-specific efficiencies (Section 5).

We simulate the model to match the evolution of U.S.-bound shipping services from 2017 to 2025 (Section 6). We rely on our empirical measure of route-specific shipping disruptions to discipline shipping productivity—the difference between potential and effective supply of shipping services. In line with the empirical evidence, we show that the entry of new shipping firms after 2020 expanded aggregate capacity, with the bulk of this increase reallocated to the Asia-West Coast route, which became increasingly profitable. This reallocation, together with falling import prices, drove a rise in the share of Asian imports.

Two counterfactual economies are constructed to measure the economic effects of shipping disruptions (Section 7). One in which the shipping productivity along the Asia to West Coast route is held constant at its initial value in February 2017. This experiment allows us to measure the impact of the port congestion at its peak in the summer of 2021. If the disruptions would not have happened, the effective supply of shipping services would have increased by 14%, imports from Asia would have reached 9.5% of aggregate output (an increase of 12%) and the relative price of Asian goods would have fell by more than 2%.

In the second experiment, the shipping productivity along the Asia to East Coast route via the Suez Canal is held constant at its initial value in February 2017. This experiment allows us to measure the impact of the attacks on container ships in the Red Sea in early 2024. The efficiency losses from the rerouting of vessels through the Cape of Good Hope were far bigger than the port congestion disruptions of 2021. The effective shipping supply would have increased by 23%, imports from Asia would have increased by 31% and the retail price of goods from Asia would have declined by 9%.

Our findings underscore the importance of understanding shipping markets not just as passive conveyors of global trade, but as strategic intermediaries whose endogenous responses to shocks can amplify or mitigate macroeconomic disruptions. This paper provides a framework to evaluate such mechanisms and offers novel data and tools for studying the intersection of trade, transportation, and macroeconomic policy.

Related literature. Much of the existing literature on maritime supply has traditionally focused on fleet capacity as the primary determinant of supply, emphasizing its constrained and inelastic nature. Notably, Stopford (2008) observes that seaborne transport supply, which is governed by merchant fleet capacity, adjusts slowly to changes in demand. This sluggish response is further highlighted by Kalouptsidi (2014), who points out that fleet capacity, constrained by high entry costs, long lead times for shipbuilding, and convex operating costs, limits the extent of supply fluctuations. Similarly, Dunn and Leibovici (2023) emphasize that global shipping supply, measured in terms of the total fleet's Twenty-Foot Equivalent Units (TEUs), remains relatively stable and largely unaffected by short-term fluctuations in global demand. Brancac-

cio, Kalouptsidi, and Papageorgiou (2024, 2025) further reveal that the supply of transportation services remains inflexible due to the rigid capacity constraints faced by both ships and ports.

However, recent disruptions such as the COVID-19 pandemic and geopolitical tensions in the Red Sea have exposed the vulnerability of maritime logistics to sudden external shocks (Alessandria, Khan, Khederlarian, Mix, and Ruhl, 2023, Notteboom, Haralambides, and Cullinane, 2024). In response, shipping companies have increasingly adapted by rerouting vessels (Notteboom, 2012) and adjusting vessel speeds (Lugovskyy, Skiba, and Terner, 2023), both of which significantly influence the actual provision of shipping services. Our paper contributes to the literature by merging these two perspectives.

2. U.S.-BOUND POTENTIAL SHIPPING SUPPLY

We begin by quantifying the evolution of potential shipping supply to the United States using high-frequency satellite data on shipping movements. Potential supply refers to the shipping services that could be delivered in the absence of disruptions, measured as the ton or ton-mile capacity implied by vessel deployments, routes, and frequencies. Using vessel-tracking data matched with ship characteristics, we construct route-level measures of potential capacity between January 2017 and March 2025. These measures capture the aggregate supply of container shipping available to U.S. importers and provide the baseline against which we later measure the efficiency losses from disruptions.

2.1. *Data*

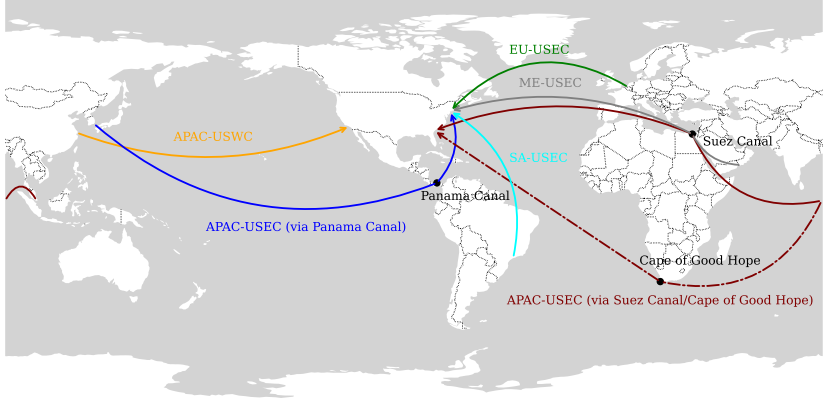
Our empirical analysis relies on two primary data sources. The first is the Automatic Identification System (AIS). Starting in 2005, the International Maritime Organization (IMO) requires all ships of 300 gross tonnage and above engaged in international trips to carry an AIS transponder capable of providing information about the vessel to other ships and coastal authorities automatically. The AIS provides high-frequency signals on vessel identity (IMO ship identification number), location, speed, and trajectory. It updates navigational data as frequently as every two seconds and produces over 2,000 reports per minute per vessel. We focus on container ships, which are the main mode of transportation for manufactured goods.[1] These data allow us to reconstruct the universe of container ship voyages arriving at U.S. ports between January 2017 and March 2025. The second is Lloyd's List vessel registry, which provides ship-level characteristics, including deadweight tonnage (DWT) and ownership. We match AIS trajectories to vessel characteristics to obtain a complete picture of ship deployments around the world.

[1] Dry bulk shipping transports bulk commodities such as iron ore, coal and grain, and oil tankers transport oil. The share of each of these in the world fleet capacity in 2024 was 43% and 28%. The remaining 30% of the world fleet capacity is in container ships and other general cargo ships (UNCTAD (2024)).

2.2. *Routes and trips*

We classify voyages into six major U.S.-bound trade routes, reflecting both geographic origin and destination, and shipping path. The six routes are: (1) Asia-Pacific to the U.S. West Coast; (2) Asia-Pacific to the U.S. East Coast via the Panama Canal; (3) Asia-Pacific to the U.S. East Coast via the Suez Canal or the Cape of Good Hope; (4) Europe to the U.S. East Coast; (5) the Middle East to the U.S. East Coast; and (6) South America to the U.S. East Coast. Figure 2.1 plots these six trade routes on a world map.

FIGURE 2.1.—Major U.S.-bound trade routes



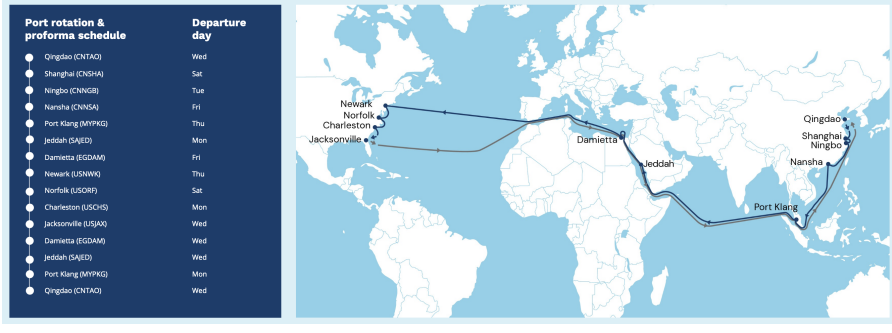
Note: The figure illustrates the approximate trajectories of the six major trade routes connecting the rest of the world to the U.S.: (1) Asia-Pacific to the U.S. West Coast (APAC–USWC); (2) Asia-Pacific to the U.S. East Coast (APAC–USEC) via the Panama Canal; (3) Asia-Pacific to the U.S. East Coast (APAC–USEC) via the Suez Canal or the Cape of Good Hope; (4) Europe to the U.S. East Coast (EU–USEC); (5) the Middle East to the U.S. East Coast (ME–USEC); and (6) South America to the U.S. East Coast (SA–USEC).

Container ships, in contrast to dry bulk vessels or tankers, typically operate on fixed service loops among predetermined sets of origin and destination ports.[2] Figure 2.2 presents an example of a predetermined trip along the Asia-Pacific to the East Coast route via the Suez Canal. Multiple ports are visited on the trip from Asia to the East Coast with specific dates for each stop. We define a trip as the journey of a vessel that begins with its departure from the last port in a foreign region of origin—namely, Asia-Pacific, Europe, the Middle East, or South America—and ends (possibly after several intermediate stops) with its arrival at the first port on either the U.S. East Coast or West Coast. In this particular example, the trip would be classified as departing from Asia (Malaysia, in particular) via the Suez Canal reaching the U.S. East Coast (namely, Newark) in about 28 days.

[2]As Brancaccio, Kalouptsidi, and Papageorgiou (2020, p.2) explain, "[t]he transportation sector . . . can be split into two categories: those that operate on fixed itineraries, much like buses, and those that operate on flexible routes, much like taxis. Container ships . . . belong to the first group."

Table 2.1 summarizes the main arrival and origin ports in our sample, including the main routes they follow and the share of trips they represent over the 2017-2025 period. We cover 646 port calls around the world as either the last port in a region of origin and the first arrival port in the U.S.. The main arrival ports in the U.S. are the ports of New York and Savannah on the East Coast and Los Angeles and Long Beach on the West Coast. The primary origin ports in the Asia-Pacific region include Busan in South Korea, Shanghai, Shenzhen, and Ningbo-Zhoushan in China; in the European region, Valencia in Spain, Bremen in Germany, and Le Havre in France; in the Middle East region, Salalah in Oman; and in the South American region, Cartagena in Colombia, and Colón in Panama.

FIGURE 2.2.—Example of a shipping route from Asia-Pacific to the East Coast



Note: The figure features the example of a route from Asia-Pacific to the East Coast via the Suez Canal. *Source:* SeaLead.

2.3. *Potential shipping supply*

The potential shipping supply measured in tons corresponds to the total DWT along a route. DWT represents the maximum weight of cargo a container ship can carry, i.e., a vessel's shipping capacity.[3] The potential supply in tons is then the sum of the shipping capacity of all container ships i operating route r in any given week t, or

$$\texttt{Potential Supply}^{\text{tons}}_{r,t} = \sum_{i \in \mathcal{I}} \mathbf{1}_{i,r,t} \times \texttt{DWT}_i, \tag{2.1}$$

where $\mathcal{I}$ denotes the set of vessels in the AIS and $\mathbf{1}_{i,r,t}$ is an indicator function that equals one when vessel i is performing a trip on trade route r during week t, and zero otherwise.

The potential shipping supply in ton-miles is the product of DWT and the average distance traveled, i.e., $\texttt{PotentialSupply}^{\text{ton-miles}}_{r,t} \equiv \texttt{Potential Supply}^{\text{tons}}_{r,t} \times \texttt{Distance}_{r,t}$. In turn, the

[3] We use DWT as the measure of shipping capacity because it is integral to the calculation of ton-miles. In contrast, Dunn and Leibovici (2023) use the total number of container ships and their capacity in twenty-foot equivalent units (TEUs) to quantify global shipping capacity.

TABLE 2.1

KEY PORTS AND U.S.-BOUND TRADE ROUTES

Rank	Destination Port	Trips (%)	Rank	Origin Port	Trips (%)	Major Routes
1	Newark (NJ)	20.0	1	Busan, South Korea	18.3	APAC–USEC (Panama), APAC–USWC
2	Los Angeles (CA)	11.1	2	Cartagena, Colombia	7.9	SA–USEC
3	Long Beach (CA)	8.7	3	Colón, Panama	6.1	SA–USEC
4	Savannah (GA)	5.7	4	Shanghai, China	5.9	APAC–USEC (Panama), APAC–USWC
5	Seattle (WA)	4.0	5	Shenzhen, China	5.5	Mostly APAC–USWC
6	Fort Lauderdale (FL)	3.9	6	Ningbo-Zhoushan, China	4.7	Mostly APAC–USWC
7	Houston (TX)	3.8	7	Valencia, Spain	4.6	EU–USEC
8	Tacoma (WA)	3.2	8	Bremerhaven, Germany	3.7	EU–USEC
9	Miami (FL)	3.2	9	Le Havre, France	3.0	EU–USEC
10	Philadelphia (PA)	3.1	10	Colombo, Sri Lanka	2.5	APAC–USEC (Suez/Cape)
11	Charleston (SC)	2.6	11	Tokyo, Japan	2.2	APAC–USEC (Panama), APAC–USWC
12	New York City (NY/NJ)	1.6	12	Yokohama, Japan	2.1	APAC–USEC (Panama), APAC–USWC
13	Norfolk (VA)	1.5	13	Kaohsiung, Taiwan	2.0	Mostly APAC–USWC
14	Boston (MA)	1.3	14	Mundra, India	1.6	APAC–USEC (Suez/Cape)
15	Port of Tampa (FL)	1.3	15	Singapore	1.6	APAC–USEC (Suez/Cape)
16	Oakland (CA)	1.3	16	Antwerp, Belgium	1.5	EU–USEC
17	Chester (PA)	0.9	17	Santa Marta, Colombia	1.5	SA–USEC
18	New Orleans (LA)	0.6	18	St. George's, Grenada	1.4	SA–USEC
19	Palm Beach (FL)	0.6	19	Xiamen, China	1.4	Mostly APAC–USWC
20	Mobile (AL)	0.5	20	Nhava Sheva, India	1.2	APAC–USEC (Suez/Cape)

Note: The third column shows the percentage of total container ship trips to each destination port listed in the second column during the sample period. Similarly, the sixth column presents the percentage of total trips originating from each origin port listed in the fifth column during the same period. The final column highlights the major routes on which trips depart from the respective origin ports and arrive at U.S. destination ports.

average distance traveled by vessels corresponds to the product of the average sailing speed along the route and time, computed as $\texttt{Distance}_{r,t} = \texttt{Speed}_{r,t} \times 24$ hours $\times$ 7 days. The average sailing speed of vessels, expressed in nautical miles per hour, on route r in week t is calculated as the DWT-weighted average

$$\texttt{Speed}_{r,t} = \sum_{i \in \mathcal{I}} \left(\frac{\mathbf{1}_{i,r,t} \times \texttt{DWT}_i}{\texttt{Potential Supply}^{\text{tons}}_{r,t}} \right) \times \texttt{Speed}_{i,t}, \tag{2.2}$$

where $\texttt{Speed}_{i,t}$ is the average speed of vessel i in week t, obtained by summing the vessel's recorded speeds in nautical miles per hour during the period divided by the number of speed measurements recorded.

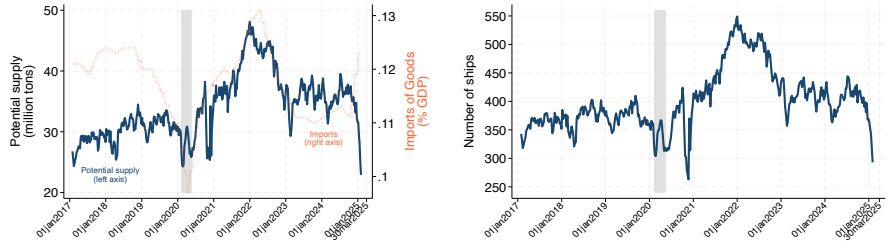
2.4. *Evolution of U.S.-bound potential shipping services*

Aggregate trends. We now analyze the evolution of U.S.-bound shipping services between January 2017 and March 2025. Panel (a) of Figure 2.3 depicts the weekly supply of shipping services. Prior to the Covid-19 pandemic, total DWT of U.S.-bound ships averaged 30 billion tons. During the post-pandemic boom, potential supply rose by more than 56% between January 2020 and January 2022. This increase reflects both the entry of new firms and the redeployment of vessels from other markets. Panel (b) of Figure 2.3 shows similar trends in the weekly number of ships en route to U.S. ports. Between 2017 and 2020, there were about 400

U.S.-bound vessels per week. That number rose by 52% between January 2020 and January 2023, peaking at 549 ships per week. This expansion coincided with a period of surging U.S. import demand and elevated shipping profits.

Both potential supply and the number of ships reverted back to values closer to the prepandemic average by mid-2023. March 2025 saw a steep decline in shipping supply in anticipation of tariffs.

FIGURE 2.3.—U.S.-bound potential shipping supply, 2017-2025



(a) Potential supply (in tons) (b) Number of Ships

Note: Panel 2.3a shows the potential supply of U.S.-bound shipping services in tons. Panel 2.3b plots the number of U.S.-bound container ships between January 2017 and March 2025.

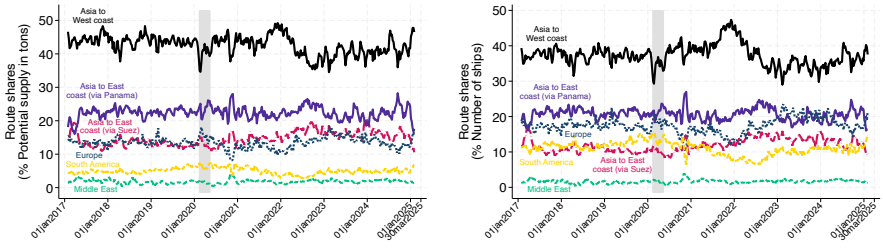
Route level reallocation. The expansion of supply was uneven across routes. The largest increase occurred on the Asia-West Coast route, which attracted the majority of new capacity after 2020. By early 2022, this route accounted for 49% of total capacity and 46% of ships—about 6 and 8 p.p. higher than their prepandemic averages (see Figure 2.4).

As the distance between Asia and the West Coast is shorter, that route was favored. Shipments from Asia to the West Coast average 2.4 weeks, while it takes approximately four weeks on average for shipments from Asia to the East Coast.[4] Although not perceptible from the plots below, the potential supply of shipping to the East Coast took longer to peak—reaching its apex in the summer of 2022.

The plots also reveal that entry played a central role in the post-2020 expansion. Through partnerships with the major shipping firms, new carriers entered the U.S.-bound market, adding vessels primarily on the Asia-West Coast route. At the same time, incumbent firms redeployed existing ships away from other markets toward U.S. trade.

[4]For shipments originating in Europe, the Middle East, and South America, the average durations are roughly 2.2, 3.0, and 2.8 weeks, respectively.

FIGURE 2.4.—U.S.-bound potential shipping supply across routes, 2017-2025



(a) Potential supply (in tons) (b) Number of Ships

Note: Panel 2.4a shows the potential supply of U.S.-bound shipping services in tons. Panel 2.4b plots the number of U.S.-bound container ships between January 2017 and March 2025.

3. DISRUPTIONS AND EFFECTIVE SHIPPING CAPACITY

While potential capacity surged after 2020, not all of it translated into effective shipping services. Port congestion, bottlenecks at the Panama and Suez Canals, and rerouting of vessels around conflict zones effectively reduced the amount of goods available to U.S. importers. We now develop novel measures of disruptions using AIS vessel-level location and speed data to capture their real-time efficiency losses. By comparing potential and effective capacity, we quantify how much supply was constrained by disruptions.

3.1. *Port congestion*

We develop a measure of port congestion based on AIS records of vessel speed and anchorage duration. Port congestion is the result of the waiting time ships endure in a designated waiting area (i.e., an anchorage) until a spot at the dock (i.e., a berth) becomes available. The more congested a port is, the longer ships have to wait. If ports were not congested, ships would proceed directly to a berth upon arrival to begin cargo operations.

We measure port congestion as the average ton-miles lost during a trip along route r in week t. We first map the geographical boundaries of berth and anchorage areas for each of the 646 container ports worldwide.[5] For each trip along a route, we consolidate the port calls of the respective vessel at the final port in the foreign region of origin, all intermediate stops, and the first port upon arrival at either the U.S. East Coast or West Coast.[6] We calculate the duration a ship spends in the anchorage areas of a port during its port calls. Let $\texttt{Port Waiting Time}_{i,p,r,t}$ denote the total number of hours vessel i spends in the anchorage areas of a port during port call p along route r in week t.

[5]We use the AIS data on container ships and the IMA-DBSCAN algorithm to do so. See Bai, Ma, Hou, Li, and Yang (2023) for details.

[6]A port call refers to the arrival of a ship at a port where it docks to load and unload cargo.

To translate this waiting time into foregone miles traveled, we multiply the waiting time by the average speed a ship would have sailed. Let $\texttt{Speed}_{i,p,r,t}$ denote the average speed vessel i would have traveled during port call p along route r in week t. It corresponds to the average speed traveled along route r net of the actual speed measured in the anchorage area, or $\texttt{Speed}_{i,p,r,t} \equiv \texttt{Speed}_{r,t} - \overline{\texttt{Speed}}_{i,p,r,t}$. Here, $\texttt{Speed}_{r,t}$ is the DWT-weighted average sailing speed of vessels along route r in week t as defined in equation (2.2). The foregone miles traveled by a vessel along a route are then multiplied by a ship's tonnage to get our measure of port congestion in ton-miles.

Our route-level measure of port congestion is given by

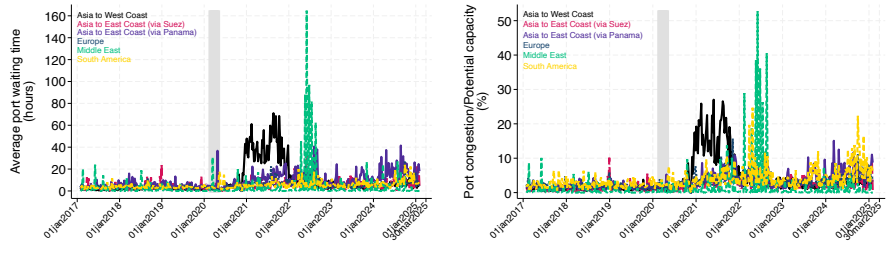
$$\texttt{Port Congestion}^{\text{ton-miles}}_{r,t} = \sum_{p \in \boldsymbol{\mathcal{P}}_r} \sum_{i \in \boldsymbol{\mathcal{I}}} \mathbf{1}_{i,r,t} \times \underbrace{\texttt{DWT}_i}_{\text{tonnage}} \times \underbrace{\texttt{Speed}_{i,p,r,t} \times \texttt{Port Waiting Time}_{i,p,r,t}}_{\text{foregone distance}}, \tag{3.1}$$

where $\boldsymbol{\mathcal{P}}_r$ denotes the set of port calls for trips along route r and $\boldsymbol{\mathcal{I}}$ the set of vessels.

Panel (a) of Figure 3.1 shows the average waiting time spent at ports for each route. Ships spent an average of 7 hours at ports across all routes over the 2017-2025 period. Due to a surge in consumer demand and pandemic-related labor shortages at the ports of Los Angeles and Long Beach, the average waiting time at ports along the Asia to West Coast route surpassed 60 hours for most part of the summer and fall of 2021 with several ships simultaneously anchored offshore. The spring of 2022 also saw a major gridlock at many ports in the Middle East, significantly impacting the Middle East to East Coast route. The port of Jebel Ali in the UAE was badly hit, experiencing prolonged berthing delays.

Panel (b) of Figure 3.1 shows our measure of port congestion as a fraction of the potential capacity in ton-miles. Port congestion reduced shipping capacity along the Asia to West coast route by as much as 27% of the potential capacity initially deployed along the route.

FIGURE 3.1.—Port congestion across routes, 2017-2025



(a) Average port waiting time (b) Port congestion/Potential supply

Note: Panel 3.1a shows the average port waiting time along the different routes. Panel 3.1b plots our measure of port congestion as a fraction of potential supply for each U.S.-bound route between January 2017 and March 2025.

3.2. *Canal congestion*

Similar to port congestion, congestion at crucial maritime chokepoints such as the Suez and Panama Canals can significantly disrupt the provision of goods en route to the U.S.. We follow the same strategy as above and reliy on AIS records of vessel speed and time to quantify the bottlenecks at the Panama and Suez Canals.

We first delineate the geographical boundaries of the Suez and Panama Canals. We then extract all AIS observations indicating that a vessel is located within these canals and moving at a speed less than 1 knot. For each of these observations, we calculate the vessel's waiting time by taking the difference between the current timestamp and the immediately preceding one. Let $\texttt{Canal Waiting Time}_{i,c,r,t}$ denote the number of hours vessel i spends waiting at the Suez or Panama Canal during its trip along route r in period t. The waiting time at canals is translated into miles using the average speed a vessel would have traveled during that amount of time. Let $\texttt{Speed}_{i,c,r,t}$ denote the speed vessel i passing through canal c along route r in period t would have traveled as $\texttt{Speed}_{i,c,r,t} \equiv \texttt{Speed}_{r,t} - \overline{\texttt{Speed}}_{i,c,r,t}$.[7] The measure of distance is converted into ton-miles by adjusting it for the ship's tonnage.

Our route-level measure of port congestion is given by

$$\texttt{Canal Congestion}^{\text{ton-miles}}_{r,t} = \sum_{p \in \boldsymbol{\mathcal{C}}_r} \sum_{i \in \boldsymbol{\mathcal{I}}} \mathbf{1}_{i,r,t} \times \underbrace{\texttt{DWT}_i}_{\text{tonnage}} \times \underbrace{\texttt{Speed}_{i,c,r,t} \times \texttt{Canal Waiting Time}_{i,p,r,t}}_{\text{foregone distance}}, \tag{3.2}$$

where $\boldsymbol{\mathcal{C}}_r$ denotes the set of AIS observations indicating vessels located in the Suez or Panama Canal with a speed less than 1 knot along route r and $\boldsymbol{\mathcal{I}}$ the set of vessels.

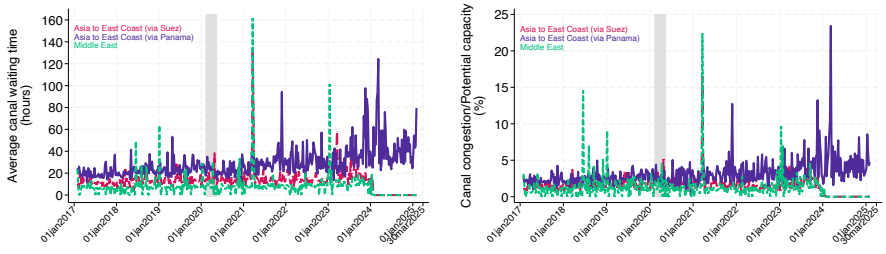
Panel (a) of Figure 3.2 shows the average waiting time at the Panama and Suez Canals for the Asia and Middle East to the U.S. East Coast routes. Ships spend significant time at the Panama and Suez canals, about 26 hours over the 2017-2025 period. Drought conditions have restricted the number of vessels that can transit the Panama Canal, while attacks on ships in the Red Sea have delayed ships passage along the Suez Canal. In particular, geopolitical unrest in the Red Sea led many shipping companies in 2024 to divert their vessels to longer and more expensive route around the Cape of Good Hope in Africa, which helps why the average canal waiting time reduced to values close to 0.

Panel (b) of Figure 3.2 shows that disruptions at the Suez Canal accounted for less than 2% of potential capacity initially deployed to the Asia and Middle East to the U.S. East Coast. In contrast, the 2023-24 drought conditions led to a significant increase in the amount time ships

[7] As before, $\texttt{Speed}_{r,t}$ is the DWT-weighted average sailing speed of vessels along route r in period t as defined in equation (2.2).

wait to cross the Panama Canal. These disruptions accounted for more than 4% of potential capacity along the Asia to East Coast route.

FIGURE 3.2.—Canal congestion across routes, 2017-2025



(a) Average canal waiting time (b) Canal congestion/Potential supply

Note: Panel 3.2a shows the average canal waiting time along the different routes. Panel 3.2b plots our measure of canal congestion as a fraction of potential supply for each U.S.-bound route between January 2017 and March 2025.

3.3. *Rerouting*

We now focus on rerouting episodes that forced vessels to divert from their planned course to a longer and/or costlier alternative to reach U.S. ports. Often in response to changing market conditions or major external events such as the Red Sea crisis in 2023, these route diversions can add significant costs to the provision of shipping services.

Using AIS tracking data, we first group trips taken by container ships along each major route according to their origin-destination (o-d) port pairs. For each o-d pair, we identify the trip with the shortest travel distance and use the shipping trajectory of the corresponding vessel as the benchmark. Let $\texttt{Min Distance}_{o,d,r}$ represent the shortest trip distance between origin o and destination d along route r. Then, for o-d pairs with multiple trajectories, we classify a trip j as rerouted if it deviates from the benchmark trajectory with the shortest trip distance. Let $\texttt{Trip Distance}_{i,j,o,d,r}$ denote vessel i's trip j distance measured in miles from origin o to destination d along route r. We adjust the additional miles traveled by the number of hours taken by the diverted route, where $\texttt{Trip Duration}_{i,j,o,d,r}$ corresponds to vessel i's trip j trip duration in hours. The additional miles per hour as a result of rerouting is then given by $\texttt{Extra Miles/Hour}_{i,j,o,d,r} \equiv \left(\texttt{Trip Distance}_{i,j,o,d,r} - \texttt{Min Distance}_{o,d,r}\right) / \texttt{Trip Duration}_{i,j,o,d,r}$. The additional miles per hour are converted to extra miles by adjusting them for the length of the period, or $\texttt{Extra Miles}_{i,j,o,d,r} \equiv \texttt{Extra Miles/Hour}_{i,j,o,d,r} \times 24\,\text{hours} \times 7\,\text{days}$.

Our route-level measure of rerouting is given by

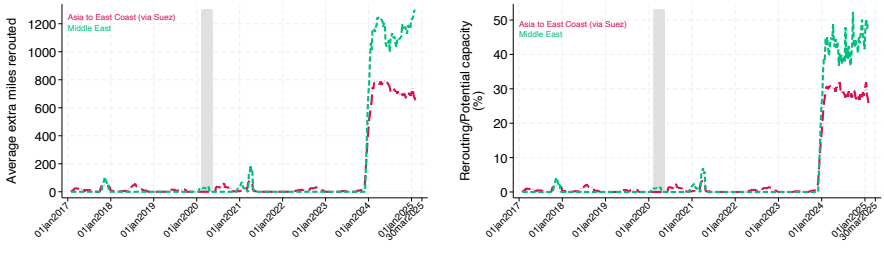
$$\texttt{Rerouting}^{\text{ton-miles}}_{r,t} = \sum_{o \in \mathcal{O}_r} \sum_{d \in \mathcal{D}_r} \sum_{j \in \mathcal{J}_{o,d,r}} \sum_{i \in \mathcal{I}} \mathbf{1}_{i,r,t} \times \underbrace{\texttt{DWT}_i}_{\text{tonnage}} \times \underbrace{\texttt{Extra Miles}_{i,j,o,d,r}}_{\text{foregone distance}}, \tag{3.3}$$

where $\mathcal{O}_r$ and $\mathcal{D}_r$ are the sets of origin and destination ports along trade route r, $\mathcal{J}_{o,d,r}$ the set of rerouted trips between origin o and destination d in route r, and $\mathcal{I}$ the set of vessels.

Panel (a) of Figure 3.3 shows the average additional distance in nautical miles resulting from the rerouting of vessels for routes that cross the Suez Canal. Although the March 2021 blockage of the Suez Canal had minimal impact on the number of vessels rerouted, the 2023 Red Sea conflict had far reaching impact. The diversion of vessels around the Cape of Good Hope added between 700 and 1,200 miles to the Asia and Middle East to the U.S. East Coast routes, raising fuel use and transit times.

Panel (b) of Figure 3.3 shows that rerouting accounted for a large fraction of the potential supply initially deployed, representing between 30 and 50% of the potential capacity.

FIGURE 3.3.—Rerouting within routes, 2017-2025



(a) Average extra miles due to rerouting (b) Rerouting/Potential supply

Note: Panel 3.3a shows the average additional miles traveled relative to the shortest distance between an origin and destination port. Panel 3.3b plots our measure of rerouting as a fraction of potential supply for each U.S.-bound route between January 2017 and March 2025.

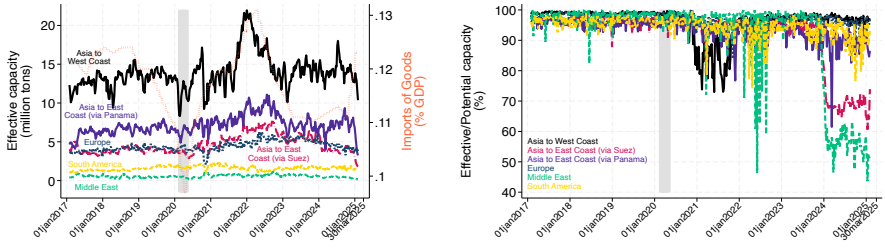
3.4. *Evolution of U.S.-bound effective shipping services*

We now combine these three measures of disruptions related to port congestion, canal bottlenecks, and rerouting into a unified measure of effective containerized shipping capacity. For each U.S.-bound route, we define effective supply as potential supply in ton-miles minus the losses implied by disruptions. We focus on effective supply in tons by dividing that measure in ton-miles by the average distance traveled.

Panel (a) of Figure 3.4 plots the evolution of effective shipping supply across routes. Despite the West Coast port congestion of 2022, effective supply still increased markedly along the

Asia to West Coast route around that period, reaching 23 million tons in January 2022. Capacity increases can also be observed in the Asia to East Coast routes, in particular by late 2022. Panel (b) of Figure 3.4 shows how much disruptions related to port congestion, canal bottlenecks, and rerouting affected the supply of shipping services.

FIGURE 3.4.—U.S.-bound effective shipping supply, 2017-2025



(a) Effective supply (tons) (b) Effective suppy/Potential supply

Note: Panel 3.4a shows the effective shipping supply in tons for each U.S.-bound route, computed as the difference between potential supply and the three measures of disruptions over the average distance of the route. Panel 3.4b plots the ratio of effective to potential supply for each U.S.-bound route between January 2017 and March 2025.

4. A MODEL OF SHIPPING WITH MULTIPLE ROUTES

The evidence in Sections 2 and 3 highlights two distinct but complementary forces in U.S.-bound shipping. On one hand, shipping firms endogenously expanded and reallocated potential capacity. On the other hand, exogenous disruptions related to port congestion, canal bottlenecks, and security issues, absorbed large shares of this capacity, sharply reducing the effective supply of shipping services that reached U.S. ports. Together, these patterns suggest that the shipping sector is neither a passive backdrop to trade nor a frictionless technology, and that the choices and constraints of shipping firms can actively shape import flows.

To interpret these patterns and quantify their implications, we now develop a multi-route general equilibrium model that embeds the two forces that shape U.S.-bound shipping: (i) the endogenous allocation of capacity across routes by profit-maximizing firms; and (ii) exogenous disruptions that reduce the delivery of shipping services. By nesting these mechanisms in a tractable general equilibrium framework, the model allows us to quantify how shocks transmit through the shipping sector to trade flows and prices, as well as to evaluate counterfactuals that are central to trade policy.

4.1. *Overview*

Consider an economy with consumers, producers, retailers, and shipping firms. In addition to domestically-produced goods, consumers enjoy foreign goods that have to be shipped from one

of the four ports of origin $o \in \mathcal{O} = \{A, E, M, S\}$ (standing for Asia, Europe, the Middle East, and South America) to one of the two arrival ports $a \in \mathcal{A} = \{E, W\}$ (standing for the East and West coasts of the United States). Imported goods from different regions are imperfect substitutes, but consumers are indifferent about the routes goods produced in the same region took to arrive in the U.S. Domestic and the bundle of imported goods are also imperfect substitutes.

Shipping firms operate a fleet of container vessels and compete across multiple U.S. bound routes $r \in \mathcal{R} = \{$*Asia to West Coast*, *Asia to East Coast via Panama Canal*, *Asia to East Coast via Suez Canal*, *Europe to East Coast*, *Middle East to East Coast*, *South America to East Coast*$\}$. In line with the empirical evidence, there is only one route and one arrival port for goods produced in Europe, the Middle East, or South America. Goods from Asia come in three different variants: they are either delivered to the East or West coast ports; and if delivered to the East coast, they can be routed through the Panama canal or the Suez canal.

Shipping firms decide how to allocate vessel capacity, what sailing speeds to adopt, and how intensively to load ships. They take the manufactured goods produced in one of the four regions to one of the destination ports along a route r. Once ships arrive at their destination, retailers purchase the goods and resell them to consumers. Retailers' sourcing decisions depend on route-specific shipping prices and idiosyncratic preferences. Time is discrete.

4.2. *Producers*

Domestic. There is a representative firm that produces domestic goods d using a linear technology in labor with productivity z_d. The firm hires domestic labor at the wage w and sells the goods directly to consumers at price p_d. The domestic firm's maximization problem requires that

$$p_d z_d = w. \tag{4.1}$$

Foreign. There are foreign firms producing goods to be exported in each origin region. These firms are willing to supply any amount of goods demanded at the price (in dollars) $\overline{p}_o$ for goods with origin in region o. The foreign producers sell their goods to retailers, but for simplicity we let the shipping firms act as intermediaries. The producers are indifferent about the routes shipping firms take and therefore do not price discriminate them (though that is an easy extension).

4.3. *Shipping firms*

Shipping market. There is a continuum of monopolistically competitive shipping firms of measure N. Each shipping firm is endowed with total capacity κ that can be optimally allocated among different routes. The capacity allocated to each route r is given by κ_r and spare capacity

(or capacity allocated to unmodeled routes) is $\overline{\kappa}$. The capacity constraint of a shipping firm can be expressed as

$$\kappa = \sum_{r \in \mathcal{R}} \kappa_r + \overline{\kappa}. \tag{4.2}$$

Shipping technology. Along each route r, shipping firms choose the average speed needed to operate their ships, s, and the amount of goods they want to transport in them or loading, ℓ, in order to produce the shipping service offered, q_r.

The technology to produce the shipping service is a function of the number of trips made along the route, $n_r(s)$, and the amount of goods transported per trip, $\ell\kappa_r$, according to

$$q_r = z_r \, n_r(s) \, \ell\kappa_r, \tag{4.3}$$

where z_r is a firm and route specific productivity term, influenced by disruptions related to the weather, strength of waves or storms, or the presence of pirates. It corresponds to the difference between potential and effective shipping supply presented in Sections 2 and 3. Here, $\ell \in [0, 1]$ is the fraction of the capacity used to transport goods. If $\ell = 0$, ships are traveling empty; if $\ell = 1$, ships are at full capacity. In turn, the number of trips made within a period evolves according to

$$n_r(s) = A_r s^{\alpha}, \tag{4.4}$$

where A_r is a route-specific efficiency term translating nautical miles per hour into number of trips and $\alpha > 0$ is a parameter. The average speed of ships is equivalent to the ratio of the distance traveled along route r, d_r, to the time traveled within the period, τ, i.e., $s \equiv d_r/\tau$. The distance along route r is exogenous and common to all shipping firms. Hence, increases in speed reduce the time traveled between origin and arrival ports.

Shipping costs. The cost of shipping goods includes the value of the goods shipped and the expenses related with transporting them. The transportation price is the wage, w.[8] The longer is the distance, the costlier it is to transport goods (e.g., it requires more fuel). The total cost of shipping along route r is

$$tc_r = \overline{p}_o(\ell\kappa_r)^{\nu} + w(n_r(s))^{\zeta}. \tag{4.5}$$

[8] As it is made clear in the definition of the equilibrium, the underlying assumption is that the shipping firms use domestic labor to operate vessels.

The cost exponents ν and ζ are such $\zeta\,(1-1/\nu)=1$. This restriction ensures the total cost function is homogeneous of degree 1 in the shipping service output.

The optimal choices of sailing speed and loading, s_r and ℓ_r, satisfy the firm's cost minimization problem, equation (4.5), subject to its shipping service technological constraint, equations (4.3) and (4.4), as well as the loading constraint $\ell \in [0,1]$. The solution to the firm's problem yields the marginal cost of shipping through route r as

$$mc_r = \frac{1}{z_r}\left(\frac{w}{1/\zeta}\right)^{1/\zeta}\left(\frac{\overline{p}_o}{1/\nu}\right)^{1/\nu}. \tag{4.6}$$

The marginal cost of shipping goods is decreasing in the shipping firm's efficiency, and increasing in the price of goods at the origin port and the wage rate.

Profits per route. A shipping firm maximizes its profits along route r by choosing the price of its shipping services, p, taking the retailers' demand for its shipping services, $\mathrm{y}_r(p)$, as given. The shipping firm's profit maximization problem for route r reads as

$$\pi_r = \max_p \left(p - mc_r\right) q_r, \tag{4.7}$$

subject to the supply of shipping services meeting its demand, i.e., $q_r = \mathrm{y}_r(p)$.

The solution to the shipping firm's problem yields a route-specific price, p_r, equivalent to a markup over the firm's marginal cost given by

$$p_r = m_r mc_r. \tag{4.8}$$

In turn, the shipping firm's markup depends on retailers' price elasticity of demand for its manufactured goods shipped through the route, $\xi_r \equiv -(\partial \mathrm{y}_r(p_r)/\partial p_r)(p_r/\mathrm{y}_r(p_r))$, according to

$$m_r = \frac{\xi_r}{\xi_r - 1}. \tag{4.9}$$

The more inelastic is the retailers' demand for goods shipped through route r (i.e., the lower is ξ_r), the higher is the shipping firm's markup.

Optimal capacity per route. The capacity allocated to each route r is chosen to maximize the shipping firm's aggregate profit, π. The aggregate profit includes the sum of profits per route across all routes net of entry costs, e, and the cost of deploying ships across routes. The latter is increasing and convex in the firm's capacity with an externality that depends on the number of competing ships sailing through the route. Let $g(K_r)$ denote a congestion factor associated

with the allocation of all ships to route r, where K_r is the market capacity allocated to route r. A shipping firm does not internalize the effect of its capacity choice on other firms' capacity.

The shipping firm's aggregate profits is given by

$$\pi = \max_{\{\kappa_r\}_{r\in\mathcal{R}}} \left\{ \sum_r \pi_r - w \sum_r g(K_r) \frac{\kappa_r^2}{2} - e \right\}. \tag{4.10}$$

subject to the capacity constraint (4.2). The shipping firm's optimal capacity per route is obtained by replacing the Lagrange multiplier on the capacity constraint in the shipping firm's first-order condition to problem (4.10), which yields the following expression

$$\kappa_r = \frac{1}{w g(K_r)} \left[(p_r - mc_r)\, z_r n_r(s_r) \ell_r - \frac{1}{|\mathcal{R}|} \sum_x (p_x - mc_x)\, z_x n_x(s_x) \ell_x \right]$$
$$+ \frac{1}{g(K_r)} \frac{1}{|\mathcal{R}|} \sum_x g(K_x) \kappa_x \tag{4.11}$$

The optimal capacity per route equates the marginal benefit of additional capacity to its marginal cost. Increasing capacity in one route raises the route's profit per ton travelled relative to the firm's average profits. However, it also increases the cost of deploying capacity to that route relative to the average. The more congested is a route, the more likely the firm is to reallocate capacity along the other routes.

Congestion. The congestion factor associated with the allocation of ships to route r depends on the aggregate capacity deployed to the route from all the competitors according to

$$g(K_r) = \varepsilon_\kappa \left(\int_0^N \kappa_r(j) dj \right)^\phi, \tag{4.12}$$

where ε_κ is a cost shifter. The larger the number of ships sailing through a route, the costlier it is for the firm to deploy its own ships.

Entrants in the shipping market. Potential shipping firms consider entering the shipping market as long as they can make profits. If a shipping firm decides to enter, it gets the expected profits from operating in the market, or $\left(\int_0^N \pi(j) dj \right) / N$. Not entering the shipping market delivers a profit of zero. The free-entry condition determines the number of shipping firms, N.

4.4. *Retailers*

There is a measure $\mathcal{I}$ of identical retailers, who specialize on goods from different regions and routes. Retailers purchase manufactured goods from a shipping firm j operating route r at

the price $p_r(j)$ and resell them to consumers at the final price p_o. The final price only depends on the origin of the goods as consumers are indifferent about the arrival port they were delivered to or the route goods took to arrive at their destination.

Technology. The output of retailers specializing on goods from route r is produced according to a decreasing returns to scale technology that aggregates all services produced by shipping firms operating along the route, with $1/(1-\sigma)$ as the elasticity of substitution, or

$$y_r = \chi_r \left(\int_0^N y_r(j)^\sigma dj \right)^{\theta/\sigma}, \tag{4.13}$$

where $\theta \in (0,1)$ is a common output elasticity and χ_r is the retailers' productivity from specializing in manufactured goods from route r.

Profits per route. Retailers' profit from each route r is given by

$$\Pi_r = \max_{\{y_r(j)\}} \left\{ p_o \chi_r \left(\int_0^N y_r(j)^\sigma dj \right)^{\theta/\sigma} - \int_0^N p_r(j) y_r(j) dj - f \right\}, \tag{4.14}$$

where $f > 0$ denotes the fixed costs of operating in the retail sector. As $\theta < 1$, retailers can make profits on some routes.

Specialization across routes. Retailers choose which shipping route r they want to source their goods from according to the following discrete choice problem

$$\Pi = \max_{r \in \mathcal{R}} \{\Pi_r + \epsilon_r\},$$

where ϵ_r are idiosyncratic taste shocks retailers have for goods from particular routes. These shocks are assumed to be mean zero Type I extreme value with scale parameter $\lambda > 0$. The optimal specialization in shipping route r is governed by the following expression

$$o_r = \frac{e^{\lambda \Pi_r}}{\sum_{x \in \mathcal{R}} e^{\lambda \Pi_x}}. \tag{4.15}$$

More profitable routes are more likely to have a larger number of retailers specializing in them.

Retailers' demand for shipped goods. It transpires that retailers' demand for manufactured goods transported through route r by a shipping firm j, $\mathrm{y}_r(j)$, is given by the quantity demanded by each retailer, $y_r(j)$, conditional on the retailer specializing on that route, o_r,

summed across all retailers, $\mathcal{I}$, according to

$$\mathrm{y}_r(j) \equiv o_r y_r(j)\mathcal{I} = o_r \left(\frac{\theta \chi_r^{\sigma/\theta} p_o y_r^{(\theta-\sigma)/\theta}}{p_r(j)} \right)^{1/(1-\sigma)} \mathcal{I}. \tag{4.16}$$

Entrants in the retail market. Potential retailers consider entering the retail market. If a firm enters the retail market, its expected profit is $\sum_{r\in\mathcal{R}} o_r \Pi_r$. If the firm decides not to enter the retail market, it gets a profit of zero. As long as profits can be made, potential entrants will join the retail sector. The free-entry condition determines the measure of retailers, $\mathcal{I}$.

4.5. *Consumers*

There is a unit measure of consumers, endowed with one unit of time. Consumers supply their unit of time inelastically in exchange for the wage rate w and receive profits Λ accrued from the portfolio of firms they own. Consumers purchase domestically-produced goods at price p_d as well as imported goods from retailers priced at p_o. The budget constraint of a consumer is given by

$$\sum_{o\in\mathcal{O}} p_o c_o + p_d d = w + \Lambda. \tag{4.17}$$

A consumer derives utility from the consumption of goods from Asia, Europe, the Middle East, and South America, c_A, c_E, c_M, and c_S, as well as domestically-produced goods d. Although goods from the same region transported along different routes are perfect substitutes, goods from different regions are not. The elasticity of substitution between them is $1/(1-\rho)$ and the bundle of imported goods can be written as

$$c = \left(\sum_{o\in\mathcal{O}} \gamma_o c_o^{\rho} \right)^{1/\rho}, \tag{4.18}$$

with γ_o denoting an origin-specific utility weight such that $\sum_{o\in\mathcal{O}} \gamma_o = 1$. Domestic goods and the bundle of imported goods are also imperfect substitutes, with their elasticity of substitution given by $1/(1-\varrho)$. The consumer's problem reads

$$u(c_A, c_E, c_M, c_S, d) = \max_{c_A, c_E, c_M, c_S, d} \left[\gamma_d d^{\varrho} + (1-\gamma_d) c^{\varrho}\right]^{1/\varrho} \tag{4.19}$$

subject to the budget constraint (4.17) and the bundle of imported goods (4.18).

4.6. *Equilibrium*

Definition (**EQUILIBRIUM**)**.** An equilibrium consists of a solution for: (1) a shipping firm's output, speed, load, capacity, price, markup, and profits, $\{q_r(j), n_r(j), s_r(j), \ell_r(j), p_r(j), m_r(j), \pi_r(j)\}$, along each route $r \in \mathcal{R}$, as well as total profits, $\pi(j)$, for all firms $j \in [0, N]$; (2) retailers' demand for goods shipped by each shipping firm j, $\mathrm{y}_r(j)$, output, y_r, corresponding profits, Π_r, and optimal decision rule o_r for each route $r \in \mathcal{R}$; (3) consumers' demand for domestically-produced goods, d, and goods from each region $o \in \mathcal{O}$, c_o; (4) the measure of shipping firms, N; (5) the measure of retailers, $\mathcal{I}$; (6) each route's shipping price, p_r, for $r \in \mathcal{R}$; (7) retail prices of goods from each region $o \in \mathcal{O}$, p_o; (8) the domestic goods price, p_d; (9) the wage rate, w; (10) the aggregate profits, Λ. These allocations are determined such that

1. Given wages, w, and goods prices at the origin port, $\overline{p}_o$, each shipping firm j maximizes its profits $\pi_r(j)$ according to (4.7), yielding a solution for $\{q_r(j), n_r(j), s_r(j), \ell_r(j), p_r(j), m_r(j)\}$ along each route r that satisfy (4.3), (4.4), (4.6), (4.8), (4.9), as well as $\ell_r(j) = \left(\frac{\zeta}{\nu}\frac{w}{\overline{p}_o}\right)^{1/\nu} n_r(j)^{\zeta/\nu}/\kappa_r(j)$. Total profits, $\pi(j)$, and the optimal capacity per route, $\kappa_r(j)$, satisfy (4.10) and (4.11).
2. Given shipping prices, p_r, and retail prices, p_o, retailers' allocations $\{y_r, \Pi_r, o_r\}$ and $\{\mathrm{y}_r(j)\}_0^N$ satisfy equations (4.13), (4.14), (4.15), and (4.16) for each route $r \in \mathcal{R}$.
3. Given the retail price of goods, p_d and p_o, wages, w, and profits, Λ, consumer demand for domestically-produced goods, d, and imported goods, c_o, from each origin $o \in \mathcal{O}$ maximize their utility (4.19) subject to the budget constraint (4.17) and the bundle of imported goods (4.18).
4. The free-entry condition for the shipping market holds according to

$$\int_0^N \pi(j)dj = 0,$$

   which determines the number of shipping firms, N.
5. The free-entry condition for the retail market holds according to

$$\sum_{r\in\mathcal{R}} o_r \Pi_r = 0,$$

   which determines the measure of retailers, $\mathcal{I}$.
6. The market between shipping firms and retailers clears in each route r so that the quantity supplied by shipping firms equates the quantity demanded by retailers (4.16), or

$$\int_0^N q_r(j)dj = o_r \left(\theta \chi_r^{\sigma/\theta} p_o y_r^{(\theta-\sigma)/\theta}\right)^{1/(1-\sigma)} \mathcal{I} \int_0^N p_r(j)^{1/(\sigma-1)} dj.$$

7. The market between retailers and consumers clears according to

$$c_A = (o_{AEP} y_{AEP} + o_{AES} y_{AES} + o_{AW} y_{AW}) \mathcal{I}$$
$$c_j = o_{jE} y_{jE} \mathcal{I} \qquad \text{for } j = \{E, M, S\},$$

   which determines the retail prices of consumer goods, $\widehat{p}_o$, from each origin $o \in \mathcal{O}$.
8. The domestic firms' problem satisfies (4.1).
9. Labor and profits from the shipping industry are rebated to consumers according to

$$w \int_0^N \sum_{r \in \mathcal{R}} \left\{ \zeta n_r(j)^{\zeta} + g(K_r) \frac{\kappa_r(j)^2}{2} \right\} dj + Ne = \theta(w + \Lambda - p_d d).$$

10. Profits in the retail market are rebated to consumers according to

$$f\mathcal{I} = (1 - \theta)(w + \Lambda - p_d d).$$

5. TAKING THE MODEL TO DATA

In this section the model is matched to U.S. data to be consistent with the shipping trends documented in Section 2. The framework features 42 parameters: 7 consumer preference parameters, $\{\rho, \varrho, \gamma_d, \gamma_o\}$ for $o \in \mathcal{O}$; 10 parameters related to retailers' problem, $\{\chi_r, \theta, \sigma, f, \lambda\}$ for $r \in \mathcal{R}$; 19 parameters related to the shipping market, $\{z_r, A_r, \alpha, \nu, \zeta, \varepsilon_\kappa, \phi, \overline{\kappa}, e\}$ for $r \in \mathcal{R}$; 4 prices of foreign good producers, $\overline{p}_o$ for $o \in \mathcal{O}$; and 1 pertaining to producers of domestic goods, z_d. The aggregate wage is the numeraire. Several of these parameters have direct data counterparts or can be normalized. Another set of parameter values can be backed out from the theory to match a set of data targets exactly and the remaining parameters are then chosen to minimize the model's prediction error relative to other targets. The set of estimated parameters is presented in Table 5.3. The targeted moments are contrasted to the data as of February 2017 in Table 5.4.

5.1. *Exogenous and externally estimated parameters*

Shipping technology and costs. The shipping productivity per route, z_r, maps directly to the ratio of effective to potential shipping supply discussed in Section 3 and presented in Figure 3.4b. The exponent on speed in the number of trips performed by container ships, α, is recovered from estimating that relationship in the data. Using satellite-based AIS data between January 2017 and March 2025, we compute the average number of trips per ship along route r

in any given month t as

$$\texttt{Number of Trips/Ship}_{r,t} = \sum_{i \in \mathcal{I}} \left(\frac{\mathbf{1}_{i,r,t} \times \texttt{DWT}_i}{\texttt{Potential Supply}^{\text{tons}}_{r,t}} \right) \times \frac{\texttt{Number of Trips}_{i,r,t}}{\sum_{i \in \mathcal{I}} \mathbf{1}_{i,r,t}},$$

and the average sailing speed along those trips as in equation 2.2. Table 5.1 presents the results from this relationship, where the number of trips per ship and average speed are measured in logs. We set the value of the exponent on speed $\alpha = 0.036$, which corresponds to the regression that includes route, year, and month fixed effects.

TABLE 5.1
NUMBER OF TRIPS AND AVERAGE SPEED

	Number of trips per vessel		
	(1)	(2)	(3)
Average sailing speed	-0.854***	0.021	0.036*
	(0.056)	(0.018)	(0.020)
Route FE	No	Yes	Yes
Year-Month FE	No	No	Yes
Observations	582	582	582
R^2	0.354	0.959	0.961

Note: Robust standard errors in parentheses. *** p<0.01, ** p<0.05, * p<0.1.

There is limited data on shipping costs by firms. We make the assumption that costs related to shipping distance are increasing and convex, and thus set the exponent $\zeta = 2$. The restriction on cost parameters, $\zeta(1 - 1/\nu) = 1$, implies that the exponent on the value of goods transported is equal to $\nu = 2$.

Congestion. The exponent on the congestion factor, ϕ, is computed by regressing the average number of hours a container ship waits in an anchorage area of a port before docking at a berth on the total number of ship visits to ports. The former is computed as

$$\texttt{Congestion Time}_{p,t} = \sum_{i \in \mathcal{I}} \left(\frac{\mathbf{1}_{i,p,t} \times \texttt{DWT}_i}{\texttt{Potential Supply}^{\text{tons}}_{p,t}} \right) \times \frac{\texttt{Number of Hours Delayed}_{i,p,t}}{\texttt{Number of Ships Delayed}_{p,t}},$$

for each port p and month t. We focus is on the top 50 global ports for trips between January 2017 and March 2025. Table 5.2 presents the results from the regression. The estimated elasticity implies a value of $\phi = 1.809$, which corresponds to the regression that includes port, year, and month fixed effects.

Retail and shipping markups. In the economy with monopolistically competitive shipping firms, the price elasticity of retailers' demand is $1/(1-\sigma)$. It transpires that the average markup of shipping firms is $1/\sigma$. A shipping firm markup of 50% is targeted, so that the underlying

TABLE 5.2

PORT CONGESTION TIME AND NUMBER OF SHIP VISITS

	Congestion time		
	(1)	(2)	(3)
# of ship visits	0.940***	1.383***	1.809***
	(0.022)	(0.083)	(0.086)
Port FE	No	Yes	Yes
Year-Month FE	No	No	Yes
Observations	4,584	4,584	4,584
R^2	0.376	0.750	0.778

Note: Robust standard errors in parentheses. *** p<0.01, ** p<0.05, * p<0.1.

elasticity of substitution is set to $\sigma = 0.667$. The marginal cost of retailers conditional on specializing on a particular route is $\theta\widehat{p}_o$. This yields a retail firm markup equal to $1/\theta$. A value of $\theta = 0.667$ is chosen, so that the corresponding average markup in retail is 50%. The value of θ is also informative about the size of the shipping and retail sector in the economy. The larger is θ, the larger the size of the shipping sector in aggregate output and the smaller the size of the retail sector.

Retail technology and specialization. Retailers' productivity across most routes can be normalized, with the exception of those from Asia. As goods from the same origin region are perfect substitutes, two of the Asian routes productivities need to be internally calibrated. Hence, we set $\chi_{AEP} = \chi_{EE} = \chi_{ME} = \chi_{SE} = 1$. The scale parameter of the mean zero Gumbel shock for retailers' specialization, λ, is normalized to $\lambda = 0.1$. Higher values of λ increase the variance of the retailers' taste shocks.

Domestic producers. The productivity of domestic producers is normalized to $z_d = 1$, which implies that the output price of domestically-produced goods equals the aggregate wage.

Consumer elasticity of substitution. Estimates of the elasticity of substitution abound. The elasticity across goods from different countries tends to be higher than the domestic vs. foreign goods elasticity as consumers are more willing to substitute imports from different countries than they are to substitute domestic for foreign goods. Feenstra et al. (2018) estimate the substitution elasticity between alternative foreign import sources (what they call the micro-Armington elasticity) and the substitution elasticity between domestic and foreign import sources (what they call the macro-Armington elasticity) using U.S. data for the 1992-2007 period. They find a micro-Armington elasticity ranging from 3.22 and 4.05, and a macro-Armington elasticity around 2 for most sectors. In line with this evidence, we set the elasticity parameter between foreign and domestically-produced goods to $\varrho = 0.5$ and the substitution parameter among imported goods to $\rho = 0.75$ (equivalent to a substitution elasticity of 2 and 4, respectively).

TABLE 5.3

PARAMETER VALUES

Parameter	Description	Value	Identification
Consumer preferences			
ϱ	Elast. of sub. between imported and domestic goods	0.500	Feenstra et al. (2018)
ρ	Elast. of sub. among imported goods	0.750	Feenstra et al. (2018)
γ_d	Cons. weight, domestic goods	0.326	Total import share
γ_o	Cons. weight, Asia, Europe, Middle East, South America	0.331, 0.295 0.127, 0.248	Regional import shares
Retail market			
χ_r	Spec. productivity, Asia to East coast via Panama/Suez/to West Coast	1.000, 0.987, 0.985	Average speed
	Europe, Middle East, South America to East Coast	1.000, 1.000, 1.000	Normalization
θ	Returns to scale	0.667	Retail markup
σ	Elast. of sub. between shipped goods	0.667	Shipping markup
f	Entry cost in retail market (/100)	3.355	Number of retail firms
λ	Scale parameter in optimal shipping route	0.100	Normalization
Shipping market			
z_r	Route productivity, Asia to East coast via Panama/Suez/to West Coast	0.959, 0.976, 0.991	Effective/Potential capacity
	Europe, Middle East, South America to East Coast	0.975, 0.969, 0.956	
A_r	Speed efficiency, Asia to East coast via Panama/Suez/to West Coast	1.019, 0.923, 1.483	DWT shares
	Europe, Middle East, South America to East Coast	1.073, 0.300, 0.648	
α	Exponent on speed	0.036	Elast. trip number wrt speed
ν	Exponent on quantity transported	2.000	Constraint
ζ	Exponent on number of trips	2.000	Normalization
ε_κ	Congestion cost shifter ($\times$1,000)	0.476	Number of shipping firms
ϕ	Congestion cost exponent	1.809	Congestion time
$\overline{\kappa}$	Idle capacity	2.469	Capacity in Asia-Europe route
e	Entry cost in shipping market	0.000	Normalization
Producers			
z_d	Productivity of domestic firms	1.000	Normalization
$\overline{p}_o$	Origin goods prices, Asia, Europe, Middle East, South America	0.735, 1.717 0.801, 2.349	Average speed

5.2. *Internally calibrated parameters*

Import shares. The consumption weights on domestically-produced goods and imported goods, $\{\gamma_d, \gamma_A, \gamma_E, \gamma_M, \gamma_S\}$, are chosen to match the total goods import share of output from the BEA in February 2017 (available here) as well as each region's import shares of merchandise trade provided by the U.S. Census Bureau for February 2017 (available here). The regional import shares correspond to the ratio of containerized vessel values over the sum of containerized vessel values from the four origin regions considered. Countries were assigned to regions following the World Bank's grouping (available here). The share of imports in aggregate output was 12.10%, the import share from Asia was 8.63%, from Europe 2.41%, from the Middle East 0.19%, and from South America 0.87%.

Given equilibrium prices and consumer elasticities of substitution, values of γ_d and $\{\gamma_o\}_{o\in\mathcal{O}}$ can be recovered to match these four targets as well as the constraint $\sum_{o\in\mathcal{O}}\gamma_o = 1$. The consumption share of output spent on domestic goods, $\omega_d \equiv p_d d/(w+\Lambda)$, can be written as

$$\omega_d = \gamma_d^{1/(1-\varrho)}\left(\frac{p_d}{P^{\text{total}}}\right)^{\varrho/(\varrho-1)},$$

and the consumption spending share on imported goods from region $o \in \mathcal{O}$, $\omega_o \equiv p_o c_o/(w + \Lambda)$, is given by

$$\omega_o = \gamma_o^{1/(1-\rho)} \left(\frac{p_o}{P^{\text{imp}}} \right)^{\rho/(\rho-1)} (1 - \omega_d).$$

Here, $P^{\text{total}} \equiv \left[\gamma_d^{1/(1-\varrho)} p_d^{\varrho/(\varrho-1)} + (1-\gamma_d)^{1/(1-\varrho)} \left(P^{\text{imp}}\right)^{\varrho/(\varrho-1)} \right]^{(\varrho-1)/\varrho}$ denotes the economy-wide price index and $P^{\text{imp}} \equiv \left(\sum_{o \in \mathcal{O}} \gamma_o^{1/(1-\rho)} p_o^{\rho/(\rho-1)} \right)^{(\rho-1)/\rho}$ the imported goods price index.

Route shares of potential capacity. Origin prices of goods from Asia, Europe, the Middle East, and South America, $\{\overline{p}_A, \overline{p}_E, \overline{p}_M, \overline{p}_S\}$, and one of the retailers' productivity from specializing in Asian goods delivered to the East coast from the Suez Canal or to the West coast, χ_{AES} or χ_{AW}, help identify the route shares of potential shipping supply in tonnage as of February 2017. The satellite-based AIS data from Section 2 are used. The route shares of the Asia to the East coast via the Panama and the Suez canals corresponded to 20.1% and 16.5% of the volume traded, Asia to the West coast represented 42.8%, and the routes from Europe, the Middle East, and South America to East coast ports were 14.5%, 1.7%, and 4.5% of the volume traded in February 2017.

The model counterpart of the route shares of potential capacity, $\varpi_r \equiv \int_0^N n_r(j)\ell_r(j)\kappa_r(j)dj / \sum_{s \in \mathcal{R}} \int_0^N n_s(j)\ell_s(j)\kappa_s(j)dj$, can be derived as

$$\varpi_r = \frac{\left(\overline{p}_{o|r}\right)^{-1/\nu} \int_0^N n_r(j)^{\zeta} dj}{\sum_{s \in \mathcal{R}} \left(\overline{p}_{o|s}\right)^{-1/\nu} \int_0^N n_s(j)^{\zeta} dj}.$$

Given cost exponents, sailing speeds, and sailing efficiencies, values of $\{\overline{p}_o\}_{o \in \mathcal{O}}$ and one of the retailers' productivity, say χ_{AES}, can be backed out to ensure the model-implied shipping route shares match the observed shares.

Average number of trips. The remaining route-specific retailer productivity, say χ_{AW}, is chosen so that the average number of trips in the model matches that in the AIS data. It takes on average between 7 (from South America) and 26 (from Asia) days to complete a U.S.-bound trip. Given that ships have an outbound voyage back to their origin regions, a ship completes on average about 1 trip per month. Retailers' productivity solves the following equation

$$\overline{n} = \frac{1}{|\mathcal{R}|} \sum_{r \in \mathcal{R}} \int_0^N n_r(j) dj.$$

Average sailing speeds. The speed efficiency shifters, $\{A_r\}_{r\in\mathcal{R}}$, are identified by the average sailing speed of vessels. The average speed along a route is derived as in equation (2.2) and relies on the AIS data presented in Section 2 as of February 2017. Vessels traveling from Asia to the East coast via the Panama and Suez canals averaged 15.0 and 15.3 knots, while those traveling from Asia to the West coast averaged 16.2 knots. The average speeds of vessels traveling from Europe, the Middle East, and South America to the East coast were 13.9, 15.7, and 11.9 knots. Given the number of trips performed in each route and the targeted sailing speeds, values of $\{A_r\}_{r\in\mathcal{R}}$ can be retrieved to ensure the average speed along a route matches the data.

Idle capacity. To compute a measure of idle capacity, we track the shipping capacity allocated to routes with origin in Asia and destination in Europe using the AIS data. Although these container ships are not the universe of vessels, they correspond to those that could potentially be reallocated to U.S.-bound routes. The share of capacity not allocated to U.S. routes corresponded to 20% of the total DWT allocated to U.S. routes in February 2017. This allows to calibrate the value of $\overline{\kappa}$.

Number of retail and shipping firms. Entry costs in the retail market, f, are calibrated so that the measure of retailers, $\mathcal{I}$, is one. Entry costs in the shipping market, e, are set to 0 and hence the congestion cost shifter, ε_κ, is chosen to match the average number of shipping firms, N, operating across the different routes. The number of shipping firms operating across the different U.S.-bound routes averaged 32 firms in February 2017.

TABLE 5.4

TARGETED MOMENTS: DATA VS. MODEL

Moment	Model	Data	Source
Import shares			
Total	0.121	0.121	BEA
Asia	0.086	0.086	Census
Europe	0.024	0.024	Census
Middle East	0.002	0.002	Census
South America	0.009	0.009	Census
Share of potential shipping supply			
Asia to East coast via Panama Canal	0.201	0.201	AIS
Asia to East coast via Suez Canal	0.165	0.165	AIS
Asia to West coast	0.428	0.428	AIS
Europe to East coast	0.145	0.145	AIS
Middle East to East coast	0.017	0.017	AIS
South America to East coast	0.045	0.045	AIS
Average sailing speeds			
Asia to East coast via Panama Canal	14.963	14.963	AIS
Asia to East coast via Suez Canal	15.276	15.276	AIS
Asia to West coast	16.223	16.223	AIS
Europe to East coast	13.887	13.887	AIS
Middle East to East coast	15.681	15.681	AIS
South America to East coast	11.862	11.862	AIS
Other targets			
Average number of trips	1.0	1.0	AIS
Average number of shipping firms	32.0	32.0	AIS
Average number of retail firms	1.0	1.0	Normalization
Idle capacity (% of DWT allocated to US-bound routes)	20.0	20.0	AIS

6. EVOLUTION OF U.S.-BOUND SHIPPING

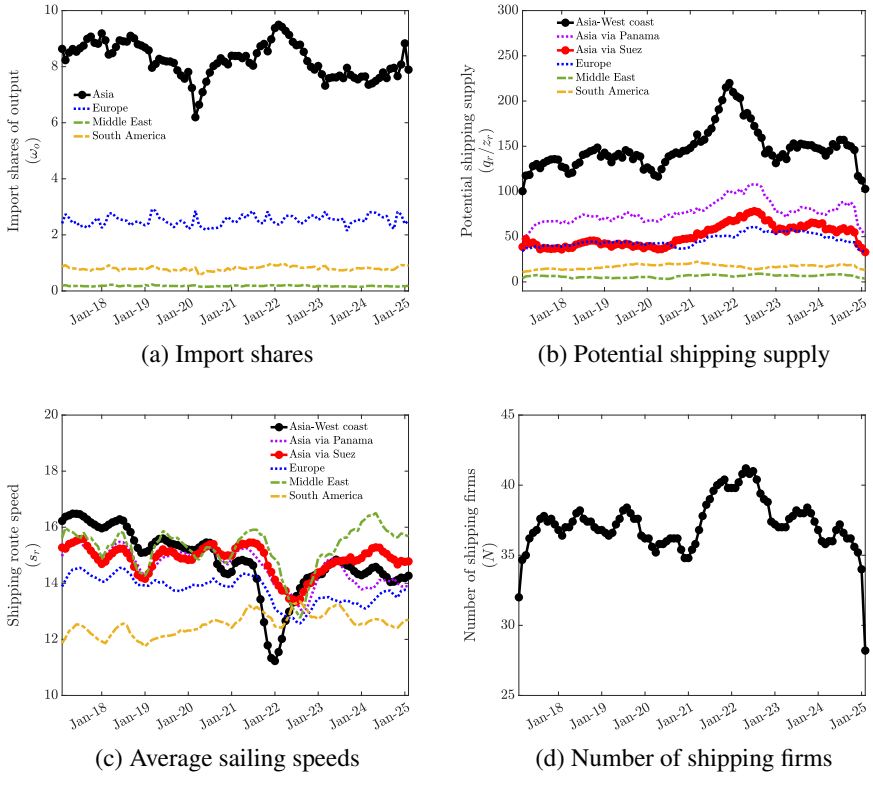
The model is now simulated to trace the evolution of import shares across regions, route shares as a fraction of potential shipping supply, average speeds, and number of firms between February 2017 and March 2025 (i.e., the variables presented in Table 5.4 above). This is achieved by solving for the values of the origin prices, speed efficiencies, congestion shocks, retailers' productivity along the routes from Asia to the East Coast via the Suez Canal and to the West Coast, and entry costs in the shipping and retail markets, $\left\{\left\{\overline{p}_{o_t}\right\}_{o\in\mathcal{O}}, \{A_{r_t}\}_{r\in\mathcal{R}}, \chi_{AES_t}, \chi_{AW_t}, e_t, f_t\right\}$. The algorithm solves for the parameter values that minimize the distance between the model-implied aggregates and the targeted data at each point in time between March 2017 and March 2025. Figure 6.1 presents the evolution of the targeted time series.

The evolution of shipping route productivities, $\{z_r\}_{r\in\mathcal{R}}$, are taken exogenously and correspond to the impact of disruptions on shipping supply, given by the times series of the ratio of effective to potential shipping supply presented in Figure 3.4b of Section 3.[9] All the other parameters are held constant over time.

[9]The time series data on potential shipping supply, average sailing speeds, number of shipping firms, and route productivities from the AIS were smoothed to reduce noise. A centered 5-month moving average was used.

The simulations help understand how the different forces shape the evolution of trade. Below, we use the model to interpret the initial impact of Covid-19 as well as the post-pandemic boom in early 2022.

FIGURE 6.1.—Targeted time series, 2017-2025



(a) Import shares

(b) Potential shipping supply

(c) Average sailing speeds

(d) Number of shipping firms

Note: Panel (a) shows the evolution of import shares of output from Asia, Europe, the Middle East, and South America in the model and the data. Panel (b) shows the evolution of potential shipping supply for the six routes in the model and the data. Panel (c) shows the evolution of average sailing speeds along the six shipping routes in the model and the data. Panel (d) shows the evolution of the number of shipping firms in the model and the data.

The Covid-19 and the blip in imports from Asia in 2020. Imports from Asia started declining in January 2020 due to the initial spread of Covid-19, bottoming out at 6.2% of output in March 2020. The pandemic caused extensive production shutdowns in China and logistical disruptions that impacted the U.S. economy. The model attributes this decline to a fall in the origin price of Asian goods, $\overline{p}_A$, with minimal disruptions from the shipping sector.

The fall of the origin price of Asian goods between February 2017 and March 2020 (about 41%) reduced the marginal cost of shipping, which allowed shipping firms to lower their Asian route prices by 23%. This reduction led to an increase in the quantity demanded of goods by retailers. On balance, the increase in quantity demanded surpassed the decline in prices, and

so retailers' variable costs increased. To raise revenues, retailers increased the arrival price of Asian goods (about 29%). The higher input espenses make specializing on Asian routes less attractive as profits from trading Asian goods fell. As a result, the fraction of retailers specializing on Asian goods routed to the West Coast or to the East Coast through the Suez Canal declined 15% and 30%. The higher retail price of Asian goods relative to other imports and domestic goods diverted consumption away from the Asian goods with households shifting a larger fraction of their expenses on domestic goods. Table 6.1 provides the magnitude of these changes.

TABLE 6.1
THE COVID-19 BLIP

		February 2017	March 2020	Δ%
Prices				
$\overline{p}_o$	Asian goods at origin	0.735	0.435	-40.8
	relative to European goods	0.428	0.170	-60.3
	relative to Middle Eastern goods	0.917	0.372	-59.4
	relative to South American goods	0.313	0.369	17.9
p_r	Shipping from Asia to East via Panama	2.682	2.066	-23.0
	Shipping from Asia to East via Suez	2.636	2.042	-22.5
	Shipping from Asia to West	2.595	2.006	-22.7
p_o/p_d	Asian goods at arrival *relative to domestic goods*	7.972	10.274	28.9
p_o/P^{imp}	*relative to imported goods index*	0.256	0.269	5.1
p_o/P^{tot}	*relative to total goods index*	0.962	1.212	26.0
Retailers specialization				
o_r	Asia to East Coast via Panama	0.181	0.186	2.8
	Asia to East Coast via Suez	0.150	0.105	-30.0
	Asia to West Coast	0.378	0.321	-15.1
	Europe to East Coast	0.199	0.281	41.2
	Middle East to East Coast	0.017	0.021	23.5
	South America to East Coast	0.074	0.086	16.2
Consumer demand				
ω_d	Domestic goods share	0.879	0.899	2.3

The post-Covid-19 boom and the rise of the Asia-West Coast route in 2021-22. The shipping sector had a far more important role in the post-Covid-19 boom. The fall in entry costs in the shipping market in late 2021 and 2022 led to an increase in the number of shipping firms (see panel 6.1d). The new entrants added more capacity to U.S. routes. In addition, shipping firms also redeployed their idle capacity to U.S.-bounds routes, further increasing capacity. Total capacity, $\sum_r \int \ell_r(j)\kappa_r(j)dj$, increased by 63% between February 2017 and January 2022. Why did firms allocate more capacity to the Asia-West Coast route? Equation (4.11) provides the intuition. Routes that are more profitable are allocated more capacity. The Asia to West Coast route is twice as profitable as the route via the Panama and three times as profitable as the route via the Suez Canal. What makes the Asia to West Coast route more profitable than the other routes from Asia to the East Coast? Despite the slowdown in sailing speeds and the resulting increase in time traveling along the Asia to West Coast route (see panel 6.1c), ship-

ping firms were able to perform more trips and load more cargo on their ships than in the other routes from Asia.

Despite the fall in prices shipping firms charged retailers, their profits from specializing on goods routed to the West Coast increased. The fraction of retailers specializing on goods from that route increased 6% at the expense of the other routes. Retailers are able to pass on the price decline of its inputs from Asia to consumers. The retail price of Asian goods declined 8%, which helps explain the increase in imports from Asia in January 2022. Table 6.2 provides additional moments from the simulation.

TABLE 6.2

THE POST-COVID-19 SURGE

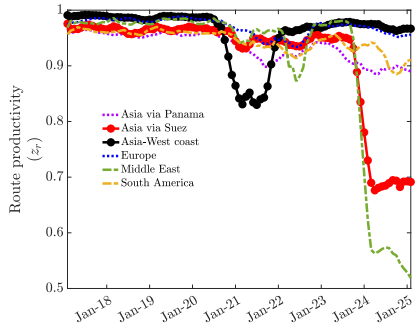
		February 2017	**January 2022**	$\Delta\%$
Shipping capacity				
$\int \ell_r(j)\kappa_r(j)dj$	Total	196.574	320.581	63.1
	Asia-East Coast via Panama route	41.931	74.529	77.7
	Asia-East Coast via Suez route	38.024	61.770	62.5
	Asia-West Coast route	61.195	109.175	78.4
Shipping profits *(relative to Middle East route)*				
π_r/π_{ME}	Asia-East Coast via Panama route	11.473	12.307	7.3
	Asia-East Coast via Suez route	9.436	8.450	-10.5
	Asia-West Coast route	24.436	26.407	8.1
	Europe-East Coast	12.645	12.150	-3.9
	South America-East Coast	4.555	4.571	0.4
Trips				
n_r	Number, Asia-East Coast via Panama route	1.123	1.313	16.9
	Number, Asia-East Coast via Suez route	1.019	1.088	6.8
	Number, Asia-West Coast route	1.639	1.923	17.3
τ_r	Days, Asia-East Coast via Panama route	24.5	26.4	7.7
	Days, Asia-East Coast via Suez route	24.9	27.0	8.2
	Days, Asia-West Coast route	11.3	16.3	44.3
Retailers specialization				
o_r	Asia to East Coast via Panama	0.181	0.190	5.0
	Asia to East Coast via Suez	0.150	0.132	-12.0
	Asia to West Coast	0.378	0.402	6.3
	Europe to East Coast	0.199	0.188	-5.5
	Middle East to East Coast	0.017	0.016	-5.9
	South America to East Coast	0.074	0.072	-2.7
Consumer demand and retail prices				
ω_d	Domestic goods share	0.879	0.871	-0.9
p_o/p_d	Asian goods at arrival *relative to domestic goods*	7.972	7.364	-7.6
p_o/P^{imp}	*relative to imported goods index*	0.256	0.254	-0.8
p_o/P^{tot}	*relative to total goods index*	0.962	0.896	-6.9

7. THE ECONOMIC EFFECT OF DISRUPTIONS

The previous section highlighted the different channels through which the shipping sector might affect the economy. To circle back to the discussion in the empirical analysis, we now focus specifically on the role of exogenous shipping disruptions. To measure the impact of shipping disruptions, we set the route productivities, z_r, to be constant throughout time, while letting the remaining exogenous drivers evolve as in the baseline simulation. We focus on two

episodes. The first relates to the months that preceded the post-pandemic boom of late 2021. Our measured disruptions during that period disproportionately affected the Asia to West Coast route as Figure 7.1 displays. The second episode studies the rerouting away from the Suez Canal due to Houthi attacks in the Red Sea in early 2024. These disruptions significantly impacted the the Asia to East Coast route via the Suez Canal and the Middle East to East Coast route.

FIGURE 7.1.—Shipping disruptions, 2017-2025



Note: The figure shows the evolution of the exogenous shipping disruptions across the different measured in Section 3.

West Coast port congestion in 2021. August through October 2021 saw a record number of ships waiting at the ports of Los Angeles and Long Beach. This unprecedented strain was not fully anticipated and put massive pressure on the shipping sector. Our micro-estimate of disruptions along the Asia to West Coast route fell by 15% in August 2021 relative to February 2017.

In this experiment, we set the shipping productivity along the Asia to West Coast route, z_{AW}, to its value in February 2017. The decline in shipping disruptions lead firms to ship goods from Asia only through the West Coast route. The improvement in shipping productivity allowed shipping firms to reduce their price (falling about 15% relative to the baseline in August 2021). Profits along the Asia to West Coast route doubled, making it the only route used by shipping firms. These firms reallocate their capacity to the Asia to West Coast route, increasing the supply of shipping services along the route. There is also a general equilibrium effect. The increase in profitability leads more shipping firms to enter the market

Since shipping firms are not operating the Asia to East Coast routes, retailers are mostly sourcing their goods from Asia through the West Coast route, concentrating close to 80% of the retail activity. Reducing disruptions would increase imports from Asia by 12% relative to the baseline in August 2021 as a result of a decline in the retail price of Asian goods relative to the price of other imports and to domestic goods. Table 7.2 provides additional details on the magnitude of the effect of disruptions associated with West Coast port congestion.

TABLE 7.1

THE WEST COAST PORT CONGESTION IN AUGUST 2021

		Baseline	No disruptions	Δ%
Effective shipping supply				
$\sum \int q_r(j)dj$	Total	361.016	403.178	13.8
	Asia-East Coast via Panama route	80.331	0	-100.0
	Asia-East Coast via Suez route	55.900	0	-100.0
	Asia-West Coast route	151.079	357.366	134.2
N	Number of shipping firms	39.600	42.623	7.6
Shipping profits (relative to Middle East route)				
π_r/π_{ME}	Asia-East Coast via Panama route	11.935	0	-100.0
	Asia-East Coast via Suez route	7.987	0	-100.0
	Asia-West Coast route	24.387	45.260	85.6
	Europe-East Coast	13.265	6.136	-53.7
	South America-East Coast	4.310	3.909	-9.3
Retailers specialization				
o_r	Asia to East Coast via Panama	0.190	0	-100.0
	Asia to East Coast via Suez	0.128	0	-100.0
	Asia to West Coast	0.384	0.797	107.6
	Europe to East Coast	0.211	0.118	-46.9
	Middle East to East Coast	0.017	0.019	11.8
	South America to East Coast	0.070	0.072	2.9
Consumer demand and retail prices				
ω_d	Domestic goods share	0.880	0.882	-0.2
ω_A	Output share of imports from Asia	0.085	0.095	11.8
p_A/p_d	Asian goods at arrival *relative to domestic goods*	8.056	7.888	-2.1
p_A/P^{imp}	*relative to imported goods index*	0.257	0.246	-4.3
p_A/P^{tot}	*relative to total goods index*	0.971	0.948	-2.4

Rerouting away from the Suez Canal in 2024. Attacks on container vessels in the Red Sea began in late 2023 and intensified throughout 2024, forcing shipping companies to reroute vessels away from the Suez Canal via the Cape of Good Hope. This added between 800 to 1,200 nautical miles to the journeys passing through the Suez Canal, corresponding to about 4 to 5 additional days of travel in our sample. Our micro-estimate of disruptions along the routes from Asia to the East Coast via the Suez Canal and from the Middle East to the East Coast fell by 31% and 42% in April 2024 relative to February 2017.

In this experiment, we set the shipping productivities along those two routes, z_{AES} and z_{ME}, to their values in February 2017. The effective shipping supply would have increased without the disruptions. This increase is driven by a reallocation of supply to the Asia to East Coast route via the Suez Canal. As before, firms would concentrate trade in one single route as shipping goods through the Suez Canal became considerably more profitable. The effect on retailers, retail prices, and consumer demand is similar to shutting down the disruptions from the West Coast port congestion of 2021. Table 7.2 provides additional details on the magnitude of the effect of disruptions in the Red Sea.

TABLE 7.2

THE SUEZ CANAL REROUTING IN APRIL 2024

		Baseline	No disruptions	Δ%
Effective shipping supply				
$\sum \int q_r(j)dj$	Total	319.316	393.867	23.3
	Asia-East Coast via Panama route	69.532	0	-100.0
	Asia-East Coast via Suez route	39.734	361.266	809.2
	Asia-West Coast route	141.211	0	-100.0
	Middle East-East Coast route	4.593	7.503	63.4
N	Number of shipping firms	36.000	36.609	1.7
Shipping profits *(relative to Middle East route)*				
π_r / π_{ME}	Asia-East Coast via Panama route	11.137	0	-100.0
	Asia-East Coast via Suez route	8.335	55.312	563.6
	Asia-West Coast route	20.555	0	-100.0
	Europe-East Coast	15.203	4.465	-70.6
	South America-East Coast	4.324	3.259	-24.6
Retailers specialization				
o_r	Asia to East Coast via Panama	0.184	0	-100.0
	Asia to East Coast via Suez	0.139	0.858	517.3
	Asia to West Coast	0.337	0	-100.0
	Europe to East Coast	0.250	0.072	-71.2
	Middle East to East Coast	0.017	0.017	0.0
	South America to East Coast	0.073	0.053	-27.4
Consumer demand and retail prices				
ω_d	Domestic goods share	0.888	0.887	-0.1
ω_A	Output share of imports from Asia	0.074	0.097	31.1
ω_M	Output share of imports from the Middle East	0.002	0.002	0.0
p_A / p_d	Asian goods at arrival *relative to domestic goods*	8.926	8.107	-9.2
p_A / P^{imp}	*relative to imported goods index*	0.262	0.240	-8.4
p_A / P^{tot}	*relative to total goods index*	1.066	0.969	-9.1
p_M / p_d	Middle Eastern goods at arrival *relative to domestic goods*	8.533	8.634	1.2
p_M / P^{imp}	*relative to imported goods index*	0.251	0.256	1.9
p_M / P^{tot}	*relative to total goods index*	1.019	1.032	1.3

8. CONCLUSION

This paper has shown that the container shipping sector actively shaped the global allocation of goods in particular in the face disruptions in 2021 and 2024. Using novel vessel-level data on all container ships arriving in the United States between 2017 and 2025, we documented two core features of the shipping market. First, potential capacity expanded sharply after 2020 but was reallocated disproportionately toward the Asia–West Coast route. Second, exogenous disruptions—port congestion, canal bottlenecks, and rerouting—absorbed a large share of this capacity, constraining effective supply precisely when global demand was strongest.

To interpret these patterns, we developed a general equilibrium model in which shipping firms act as a key intermediary in trade, by reallocating capacity across different routes, choosing sailing speeds and loading factors when faced with exogenous disruptions. Calibrated to micro data, the model replicates the key empirical facts and yields two main insights. First, entry and capacity reallocation can either amplify or dampen global trade imbalances: shipping firms endogenously channel resources toward the most profitable routes. Second, disruptions magnify volatility by tightening capacity in high-demand periods, raising prices. Taken to-

gether, these findings recast container shipping as a strategic intermediary that transmits and amplifies global shocks.

REFERENCES

G. Alessandria, S. Y. Khan, A. Khederlarian, C. Mix, and K. J. Ruhl. The Aggregate Effects of Global and Local Supply Chain Disruptions: 2020–2022. *Journal of International Economics*, 146:103788, 2023. [3]

X. Bai, Z. Ma, Y. Hou, Y. Li, and D. Yang. A Data-Driven Iterative Multi-Attribute Clustering Algorithm and Its Application in Port Congestion Estimation. *IEEE Transactions on Intelligent Transportation Systems*, 24:12026–12037, 2023. ISSN 1558-0016. [8]

X. Bai, J. Fernández-Villaverde, Y. Li, and F. Zanetti. The Causal Effects of Global Supply Chain Disruptions on Macroeconomic Outcomes: Evidence and Theory. Working Paper 32098, National Bureau of Economic Research, 2024. []

X. Bai, J. Fernández-Villaverde, Y. Li, L. Xu, and F. Zanetti. The (Un)Intended Consequences of Oil Sanctions Through the Dark Shipping of Sanctioned Oil. Working Paper 33486, National Bureau of Economic Research, 2025. []

J. Blaum, F. Esposito, and S. Heise. Input Sourcing Under Climate Risk: Evidence From U.S. Manufacturing Firms. Technical report, SSRN, 2024. []

G. Brancaccio, M. Kalouptsidi, and T. Papageorgiou. Geography, Transportation, and Endogenous Trade Costs. *Econometrica*, 88(2):657–691, 2020. [4]

G. Brancaccio, M. Kalouptsidi, and T. Papageorgiou. Investment in Infrastructure and Trade: The Case of Ports. Working Paper 32503, National Bureau of Economic Research, 2024. [2]

G. Brancaccio, M. Kalouptsidi, and T. Papageorgiou. Rigidities in Transportation and Supply Chain Disruptions. *AEA Papers and Proceedings*, 2025. Forthcoming. [3]

J. Dunn and F. Leibovici. Navigating the Waves of Global Shipping: Drivers and Aggregate Implications. Working Paper 2023-002, Federal Reserve Bank of St. Louis, 2023. [2, 5]

R. C. Feenstra, P. Luck, M. Obstfeld, and K. N. Russ. In search of the armington elasticity. *The Review of Economics and Statistics*, 100(1):135–150, 2018. [23, 24]

I. Heiland, A. Moxnes, K. H. Ulltveit-Moe, and Y. Zi. Trade From Space: Shipping Networks and the Global Implications of Local Shocks. Technical Report 14193, Centre for Economic Policy Research, 2019. []

M. Kalouptsidi. Time to Build and Fluctuations in Bulk Shipping. *American Economic Review*, 104(2):564–608, 2014. [2]

V. Lugovskyy, A. Skiba, and D. Terner. Unintended Consequences of Environmental Regulation of Maritime Shipping: Carbon Leakage to Air Shipping. Working paper, SSRN, 2023. [3]

T. Notteboom, H. Haralambides, and K. Cullinane. The Red Sea Crisis: Ramifications for Vessel Operations, Shipping Networks, and Maritime Supply Chains. *Maritime Economics & Logistics*, 26(1):1–20, 2024. [3]

T. E. Notteboom. Towards a New Intermediate Hub Region in Container Shipping? Relay and Interlining via the Cape Route vs. The Suez Route. *Journal of Transport Geography*, 22:164–178, 2012. [3]

M. Stopford. *Maritime Economics*. Routledge, London, 3 edition, 2008. ISBN 978-0-429-23954-0. . [2]

UNCTAD. Review of maritime transport 2024. UNCTAD, 2024. [3]

W. Y. Yap and D. Yang. Geopolitical Tension and Shipping Network Disruption: Analysis of the Red Sea Crisis on Container Port Calls. *Journal of Transport Geography*, 121:104004, 2024. []